SLAC–PUB–3400
SLAC/AP–37
December 1984
(A/AP)

COHERENT BEAM-BEAM INSTABILITY IN COLLIDING BEAM STORAGE RINGS*

A. W. CHAO AND R. D. RUTH

Stanford Linear Accelerator Center
Stanford University, Stanford, California, 94305

ERRATUM

One must be very careful with references. When we mentioned the "familiar effect of the dynamic β" (page 7) and then again the "dynamic tune" (page 11), we referred to

15. F. Amman and D. Ritson, International Conference on High Energy Accelerators, Brookhaven National Laboratory, 1961, p. 471.

However, John Rees has pointed out that the above reference is incorrect. The dynamic β was realized a few years later, and the correct references are:

15. F. Amman, R. Andreani, M. Bassetti, M. Bernardini, A. Cattoni, R. Cerchia, V. Chimenti, G. Corazza, E. Ferlenghi, L. Mango, A. Massarotti, C. Pellegrini, M. Placidi, M. Puglisi, G. Renzler, F. Tazzioli, International Conference on High Energy Accelerators, Dubna USAEC Conf–114 (1963) p. 309.
16. B. Richter, Proc. International Symposium on Electron and Positron Storage Rings, Saclay (1966) p. I-1-1.

We would like to thank John Rees for pointing out this error, and we would like to apologize to the authors involved for our oversight.

* Work supported by the Department of Energy, contract DE – AC03 – 76SF00515.

SLAC–PUB–3400
SLAC/AP-37
August 1984
(A/AP)

Coherent Beam-Beam Instability in Colliding Beam Storage Rings*

A. W. CHAO AND R. D. RUTH

Stanford Linear Accelerator Center
Stanford University, Stanford, California, 94305

Submitted to *Particle Accelerators*

* Work supported by the Department of Energy, contract DE – AC03 – 76SF00515.

1. Introduction

In a colliding beam storage ring, the motion of particles in one beam is strongly perturbed at the collision points by the electromagnetic field associated with the counter-rotating beam. This beam-beam perturbation leads to a stability limit on the beam intensities which is one of the most severe limits on the achievable luminosity in storage rings.

The simplest and most familiar way of describing the beam-beam problem is provided by the strong-weak picture in which one of the beams (the strong beam) is regarded as rigid, i.e. unperturbed by the presence of the other (weak) beam. As far as the weak beam motion is concerned, the strong beam acts as a nonlinear lens located at the collision points. The weak beam then circulates around the storage ring, periodically perturbed by the static nonlinear force due to the strong beam.

The strong-weak picture of the beam-beam interaction has provided useful insight into the mechanism of the beam-beam instability. It is, however, only a limited view of the beam-beam interaction. In fact it has been pointed out by several authors[1–9] that the identification of the beam-beam instability with instabilities in a periodic nonlinear mapping can not completely represent the physics of two strong colliding beams. Experimentally, the existence of beam-beam coherent dipole motion is well established.[10,11] One can also argue that the DCI experience[12] indeed indicates that coherent effects play a dominant role in determining beam-beam behavior.

In this paper, we analyze the coherent beam-beam effects of colliding beams using the Vlasov technique. The distributions ψ_1 and ψ_2 of the two beams influence each other according to the Vlasov equation, which is linearized for small perturbations $\Delta\psi_1$ and $\Delta\psi_2$ around the equilibrium distribution ψ_0. The perturbations $\Delta\psi$'s transform simply by a rigid rotation in the phase space as the beams circulate around the storage ring and then receive sudden changes at the collision points due to the beam-beam interaction. After linearization, the motion of $\Delta\psi$'s can be solved by a matrix technique which will be discussed in more detail later.

We find that there are coherent beam-beam instabilities when ν=rational number (ν is the betatron tune) similar to the resonance instabilities found in the incoherent motions of the strong-weak picture. The widths of the coherent resonances, however, tend to be larger than the corresponding resonance widths for the incoherent case. The coherent beam-beam effects therefore set a more stringent beam-beam stability threshold against nonlinear resonances than the incoherent strong-weak effects. We therefore follow the previous authors and suggest once again that coherent effects play a dominant role in the complex beam-beam phenomena.

The reason that coherent effects set a tighter stability limit than incoherent effects is basically the following. In coherent motions, the separation between one piece of the beam and the corresponding piece of the counter-rotating beam is effectively twice the separation of the strong-weak case in which one of the beams does not move. As a result, the beam-beam kicks are effectively stronger for coherent motions. The simplest example of this effect can be seen by considering two colliding bunches each with a rigid uniform disk distribution of charge. There are two coherent modes of dipole motions of the two bunches, one with each bunch moving up and down in phase and the other out of phase. The in-phase mode is always stable since the beam-beam force has no coherent effect when the bunches move up and down together. The out-of-phase mode on the other hand has a stability limit that is twice as stringent as the case when only one of the two bunches moves. This is illustrated in Fig. 1(a). The situation is even more pronounced when there is more than one bunch per beam. The rigid bunch model can be carried out for multiple bunches as well, yielding results shown in Figs. 1(b)-(d).[2-4] In each plot, the dotted line shows the boundary of stability determined by the strong-weak consideration. The fact that the coherent effects set a tighter stability limit than the incoherent effects is apparent from these plots.

2. The Vlasov Technique

We first consider the case in which each colliding beam consists of a single bunch of particles. The bunches are assumed to have a flat distribution like a horizontal ribbon at the collision points. The bunch motions occur only in the vertical y-direction. Let $\psi_{1,2}(y,y')$ be the distribution functions of the two bunches satisfying the normalization conditions

$$\begin{gathered}\int_{-\infty}^{\infty} dy' \, \psi_{1,2}\,(y,y') = \rho_{1,2}(y) \\ \int_{-\infty}^{\infty} dy \rho_{1,2}(y) = 1\end{gathered} \tag{1}$$

where $\rho_{1,2}$ are the spatial distributions of the two bunches. We assume the two bunches have the same number of particles N.

A particle in beam 1 with vertical displacement y at the collision point experiences a beam-beam kick from the electromagnetic field of beam 2 given by

$$\Delta y' = -\frac{4\pi\, N\, r_e}{L_x\, \gamma} \int_{-\infty}^{\infty} d\bar{y}\; \rho_2(\bar{y})\; H_1(y-\bar{y}) \tag{2}$$

where r_e is the classical radius of the electron, L_x is the horizontal width of the ribbon beams at the collision points, γ is the relativistic Lorentz factor and

$$H_1\,(x) = \begin{cases} 1 & \text{if } x > 0 \\ -1 & \text{if } x < 0 \end{cases} \quad . \tag{3}$$

We have assumed that the beam particles are electrons in one beam and positrons in the other beam. The reason for the H_1 function is that particles in beam 2 located at $\bar{y} > y$ kick the test particle in beam 1 upward while particles with $\bar{y} < y$ kick the test particle downward. A similar expression holds for the kicks received by particles in beam 2 from fields of beam 1.

The Vlasov equations that describe the motion of $\psi_{1,2}$ are given by

$$\frac{\partial\psi_1}{\partial s} + y'\frac{\partial\psi_1}{\partial y} - \left[K(s)y + \frac{4\pi\,N\,r_e}{L_x\gamma}\delta_p(s)\int_{-\infty}^{\infty} d\bar{y}\;\rho_2(\bar{y})\,H_1(y-\bar{y})\right]\frac{\partial\psi_1}{\partial y'} = 0 \tag{4}$$

together with another equation with indices 1 and 2 exchanged. In Eq.(4), $K(s)$ is the focusing gradient function around the storage ring, s is the distance along the orbit, and $\delta_p(s)$ is the periodic δ-function representing the periodic beam-beam perturbations. The period of $\delta_p(s)$ is the distance between collision points L.

The beam collisions perturb the focusing structure in the storage ring so that at equilibrium both beams have a distorted distribution $\psi_0(y, y')$ satisfying

$$\frac{\partial\psi_0}{\partial s} + y'\frac{\partial\psi_0}{\partial y} - F(y,s)\,\frac{\partial\psi_0}{\partial y'} = 0 \tag{5}$$

where

$$F(y,s) = K(s)y + \frac{4\pi\,N\,r_e}{L_x\gamma}\delta_p(s)\int_{-\infty}^{\infty} d\bar{y}\,H_1(y-\bar{y})\int_{-\infty}^{\infty} d\bar{y}'\,\psi_0(\bar{y},\bar{y}')$$

Note that ψ_0 is a periodic function of s with period L; it gives the equilibrium distribution of both beams in the distorted beam-beam potential-well. When observed at a fixed location in the storage ring, ψ_0 is static in time.

We are not interested in the static behavior of the beam distributions in this work. The motions that interest us are the time dependent dynamic motion of the beam distributions around the equilibrium distribution ψ_0. In particular, if we let

$$\psi_{1,2} = \psi_0 + \Delta\psi_{1,2} \tag{6}$$

with infinitesimal $\Delta\psi_{1,2}$, we would like to know under what conditions the perturbations grow exponentially in time. When these conditions are satisfied, coherent beam-beam instability occurs.

Substituting Eq. (6) into Eq. (4) and keeping only the first order terms in $\Delta\psi$'s, we obtain the linearized Vlasov equations

$$\frac{\partial f_\pm}{\partial s} + y' \frac{\partial f_\pm}{\partial y} - F(y,s)\,\frac{\partial f_\pm}{\partial y'}$$

$$\mp\ \frac{\partial \psi_0}{\partial y'}\,\frac{4\pi N r_e}{L_x \gamma}\,\delta_p(s) \int_{-\infty}^{\infty} d\bar{y}\, H_1(y-\bar{y}) \int_{-\infty}^{\infty} d\bar{y}' f_\pm(\bar{y},\bar{y}',s) = 0 \tag{7}$$

where we have defined

$$f_\pm = \Delta\psi_1 \pm \Delta\psi_2 \quad . \tag{8}$$

Note that the two functions f_+ and f_- are decoupled. They define a " $+$ " and a " $-$ " mode in the motion of the two colliding bunches.

Since we are not interested in finding the actual ψ_0 in the distorted potential well, we assume that

$$F(y,s) \cong F(s)y \quad , \tag{9}$$

i.e., the equilibrium part of the beam-beam force is approximately linear in y. Such a treatment is a familiar one in the problem of longitudinal instability in storage rings.[13] The static part of the beam-beam force is thus included simply as a perturbation to the linear focusing structure of the storage ring.

Equation (7) is the Vlasov equation written in Cartesian coordinates y and y'. We now make a transformation to the polar (action-angle) coordinates of betatron oscillations,[14] J and ϕ,

$$y = \sqrt{2\beta J}\ \cos\phi$$

$$y' = -\sqrt{\frac{2J}{\beta}}\ (\sin\phi - \frac{\beta'}{2}\ \cos\phi) \tag{10}$$

where the betatron phase ϕ and the betatron function β are derived using the focusing function $F(s)$ instead of the unperturbed $K(s)$. Note that the static perturbation of the focusing structure of the storage ring may make the linear incoherent motion unstable; this leads to the familiar effect of the dynamic β[15] and is the origin of the dotted lines in Fig. 1.

Assuming that the incoherent motion with the focusing function $F(s)$ is stable, and that we can indeed make the transformation in Eq. (10), then the equilibrium distribution ψ_0 is a function only of J

$$\psi_0 = \psi_0(J) \quad . \tag{11}$$

In these coordinates the Vlasov equations become

$$\begin{aligned} &\frac{\partial f_\pm}{\partial s} + \frac{1}{\beta}\frac{\partial f_\pm}{\partial \phi} \pm \psi_0'(J)\ \sqrt{2\beta J}\sin\phi \frac{4\pi N r_e}{L_x \gamma}\ \delta_p(s) \\ &\times \int_{-\infty}^{\infty} d\bar{y}\ H_1(y-\bar{y}) \int_{-\infty}^{\infty} d\bar{y}' f_\pm(\bar{y},\bar{y}',s) = 0 \quad . \end{aligned} \tag{12}$$

3. Solving the Vlasov Equation

To proceed, we will choose a simple model of ψ_0, the water-bag model:

$$\psi_0(J) = \frac{1}{\pi\epsilon} H(\epsilon/2 - J) \tag{13}$$

where $H(x)$ is the Heaviside step function, $H(x) = 1$ if $x > 0$ and $H(x) = 0$ if $x < 0$, and ϵ is the vertical emittance of the equilibrium beam distribution.

To be perfectly self-consistent, ψ_0 would have to give a beam-beam kick linear in y as assumed in Eq. (9). Such a distribution does exist and is given by

$$\psi_0(J) = \frac{1}{2\pi\sqrt{2\epsilon}} \frac{1}{\sqrt{\epsilon/2 - J}} \qquad (J < \epsilon/2) \quad . \tag{14}$$

As we explained before, however, perfect self-consistency is not what we need to describe the dynamic behavior of the beam-beam system; the mathematical simplicity of the water-bag model makes it more suitable for our purpose.

By inspection, the distribution perturbations can be written for the water-bag model as

$$f_\pm(J,\phi,s) = \delta(J-\epsilon/2)\sum_{\ell=-\infty}^{\infty} g_\ell^\pm(s)\, e^{i\ell\phi} \quad . \tag{15}$$

The $\delta(J-\epsilon/2)$ factor represents the fact that the perturbations occur only at the edge of the water-bag. We have also decomposed the angular part of the distribution into a Fourier series in ϕ. For simpler notation, we will drop the $+$ and $-$ superscripts on g_ℓ's in the subsequent expressions.

Substituting Eqs. (13) and (15) into the Vlasov equation (12) gives an infinite set of equations describing the coupled motion of the Fourier components $g_\ell\ (s)$ for all ℓ:

$$\frac{\partial g_\ell}{\partial s} + \frac{i\ell}{\beta} g_\ell \mp \frac{2N\,r_e}{\pi\,L_x\gamma}\sqrt{\frac{\beta}{\epsilon}}\,\delta_p(s)\sum_{k=-\infty}^{\infty} \mathcal{M}_{\ell k}\, g_k = 0 \tag{16}$$

where we have defined a matrix $\mathcal{M}$ with elements given by

$$\begin{aligned}\mathcal{M}_{\ell k} &= \int_0^{2\pi} d\phi\, e^{-i\ell\phi}\sin\phi \int_0^{2\pi} d\bar\phi\; H_1(\cos\phi-\cos\bar\phi)\, e^{ik\bar\phi} \\ &= \begin{cases} \dfrac{-32i\ell}{[(\ell+k)^2-1]\,[(\ell-k)^2-1]} & \text{if } \ell+k=\text{even} \\ 0 & \text{if } \ell+k=\text{odd} \end{cases}\end{aligned} \tag{17}$$

The matrix $\mathcal{M}$ has the following properties:

$$\begin{aligned} \mathcal{M} &= \text{purely imaginary} \\ \mathcal{M}^2 &= 0 \\ \mathcal{M}_{\ell,-k} &= \mathcal{M}_{\ell k} \\ \mathcal{M}_{-\ell,k} &= -\mathcal{M}_{\ell k} \quad . \end{aligned} \tag{18}$$

Between collisions, the different g_ℓ's are decoupled. A particular g_ℓ transforms by

$$g_\ell(L^-) = g_\ell(0^+)\ e^{-i\ell\mu} \tag{19}$$

with

$$\mu = \int_0^L \frac{ds}{\beta(s)} \ .$$

Thus μ is the integrated betatron phase from one collision point to the next, and L is the distance between collision points. The superscripts $+$ and $-$ in the arguments of g_ℓ refer to immediately after and immediately before the beam-beam collisions respectively.

The beam-beam action is obtained by integrating Eq. (16) through $s = 0$, which yields

$$g_\ell(0^+) - g_\ell(0^-) = \pm \frac{2Nr_e}{\pi L_x \gamma} \sqrt{\frac{\beta^*}{\epsilon}} \sum_k \mathcal{M}_{\ell k} g_k(0^-) \tag{20}$$

where β^* is the value of the betatron function at the collision point in the presence of the static beam-beam force. Note that we have used $g_k(0^-)$ on the right hand side of Eq. (20). Using $g_k(0^+)$ would give the same result since $\mathcal{M}^2 = 0$.

Eqs. (19) and (20) can be combined to give the matrix transformation on the vector

$$\begin{bmatrix} \vdots \\ g_2 \\ g_1 \\ g_0 \\ g_{-1} \\ g_{-2} \\ \vdots \end{bmatrix} \tag{21}$$

from one collision point to the next. This transformation is given by

$$T = R \left(I \pm \frac{2\,N\,r_e}{\pi\,L_x\,\gamma} \sqrt{\frac{\beta^*}{\epsilon}}\ \mathcal{M} \right) \tag{22}$$

where

$$R = \begin{bmatrix} \ddots & & & & & \\ & e^{-2i\mu} & & & \text{\huge 0} & \\ & & e^{-i\mu} & & & \\ & & & 1 & & \\ & \text{\huge 0} & & & e^{i\mu} & \\ & & & & & e^{2i\mu} \\ & & & & & & \ddots \end{bmatrix}$$

is the diagonal matrix describing the action between collision points, and I is the identity matrix.

4. Coherent Beam-Beam Instability

In the absence of beam-beam collisions, Eq. (22) gives the unperturbed transformation $T = R$. The eigenvalues of T are

$$\lambda = e^{-i\ell\mu}, \quad \ell = 0, \pm 1, \pm 2, \cdots \tag{23}$$

corresponding to the motion of the ℓ^{th} Fourier component of the distributions. All eigenvalues have absolute value of unity provided that the focusing structure $F(s)$ yields stable oscillations.

As the beam-beam strength is increased, the eigenvalues are more and more perturbed. A coherent instability occurs when any one of the eigenvalues acquires an absolute value larger than unity.

The coherent instability is most pronounced when the betatron phase advance between collision points is close to a rational number times π, i.e.

$$\nu = \frac{\mu}{\pi} \approx \frac{m}{\ell} \tag{24}$$

where ν is the total betatron tune of the storage ring. Close to the resonance condition (24) the Fourier components that perturb the beam motion most are

g_ℓ and $g_{-\ell}$. Keeping only the ℓ^{th} and the $(-\ell)^{th}$ elements in the transformation matrices (22) and defining the small distance between ν and m/ℓ to be

$$\Delta = \nu - \frac{m}{\ell} \quad , \tag{25}$$

the matrix T becomes

$$T = \begin{bmatrix} (1 \pm i\alpha)\ e^{-i2\pi\ell\Delta} & \pm i\alpha\ e^{-i2\pi\ell\Delta} \\ \mp i\alpha\ e^{i2\pi\ell\Delta} & (1 \mp i\alpha)\ e^{i2\pi\ell\Delta} \end{bmatrix} \tag{26}$$

with

$$\alpha = \frac{32\ell}{4\ell^2 - 1} \cdot \frac{2Nr_e}{\pi L_x \gamma} \sqrt{\frac{\beta^*}{\epsilon}}$$

The eigenvalues of (26) are then determined by the secular equation

$$\lambda^2 - 2\lambda[\cos 2\pi\ell\Delta \ \pm \ \alpha \sin 2\pi\,\ell\Delta] + 1 = 0 \tag{27}$$

One of the eigenvalues has absolute value larger than unity and therefore the beam-beam system is unstable if

$$|\cos\ 2\pi\ell\Delta \ \pm \ \alpha \sin 2\pi\ell\Delta| \quad > \ 1 \ . \tag{28}$$

The $+$ and $-$ signs in Eq. (28) refer to the f_+ and f_- modes defined in Eq. (8).

Before we interpret Eq. (28), we need to calculate the dynamic tune ν, remembering that the static beam-beam force has modified the focusing structure of the storage ring. Using the water-bag distribution, the focusing structure $F(s)$ is found from Eq.(5) to be

$$F(y,s) = K(s)y + \frac{8Nr_e}{L_x\gamma}\ \delta_p(s)\left[sin^{-1}\left(\frac{y}{\sqrt{\beta^*\epsilon}}\right) + \frac{y}{\sqrt{\beta^*\,\epsilon}}\sqrt{1 - \frac{y^2}{\beta^*\,\epsilon}}\right] \tag{29}$$

The average tune shift due to the second term in Eq. (29) is given by its detuning contribution evaluated at the amplitude $J = \epsilon/2$, that is, at the edge of the water-bag. The dynamic tune ν[15] to first order in the beam-beam strength is found to satisfy

$$\cos 2\pi\nu = \cos 2\pi\nu_0 - \frac{64}{3\pi}\,\frac{Nr_e}{L_x\gamma}\sqrt{\frac{\beta^*}{\epsilon}}\,\sin 2\pi\nu_0 \tag{30}$$

where ν_0 is the betatron tune in the absence of the static beam-beam force. Note that the tune shift is evaluated at $J = \epsilon/2$ rather than at $J = 0$ (small y). This yields a tune shift which is $8/3\pi$ times smaller.

Equation (28) determines the instability region near the resonance $\nu = m/\ell$ with a resonance stop band width approximately given by

$$\delta\nu_\ell \approx \frac{1}{2\pi}\cdot\frac{32}{4\ell^2-1}\;\xi \tag{31}$$

where we have defined a beam-beam strength parameter

$$\xi = \frac{4Nr_e}{\pi L_x\gamma\sqrt{\epsilon/\beta^*}} \tag{32}$$

which is the tune shift parameter defined in strong-weak beam-beam motion. The stop band centers around $\nu = m/\ell$. The '+' mode is unstable on the side $\nu > m/\ell$ while the '$-$' mode is unstable on the other side.

The higher order resonance stop bands ($\ell > 1$) are affected by the tune shift (30) only in that their postions are shifted as the beam-beam strength is increased. On the other hand, for the lowest order resonance $\ell = 1$, the instability condition in (28) for the $+$ mode becomes $|\cos 2\pi\nu_0| > 1$. This means that if the incoherent motion is stable (ν_0 defined), the '+' mode coherent motion will also be stable. The instability condition for the '+' mode is thus eliminated while the instability strength for the '$-$' mode is essentially doubled.

The results of this study are most conveniently shown by the instability diagrams in the two scaling parameters ν and ξ. The ℓ^{th} order resonance will then be apparent from the unstable region that originates from the tune value $\nu = m/\ell$ in these diagrams.

Figures 2(a)-(d) give the numerical results of the coherent beam-beam instability for the case of one particle bunch per beam. As the higher and higher order resonances are included, the stability diagram becomes more and more complicated. In these numerical calculations, we have used the matrix in Eq.(22) truncated to the order of resonance we consider. The results in general agree quite accurately with the approximate expression in Eq.(28) except for the weak modifications resulting from the interference between adjacent resonances. Figure 3 shows the instability diagram when resonances up to the 5th order are included. The region indicated by a box in Figure 3(a) is blown up in Figure 3(b) to show the interference between a 3^{rd} order and a 5^{th} order resonance. For practical purposes, however, these details are not very important.

5. Multiple Bunches

So far we have studied the case in which there is only one particle bunch in each beam. As we will show in this section, the Vlasov technique can also be extended to treat M bunches per beam in a storage ring with $2M$ collision points spaced by the distance L.

We assume all bunches are equally populated with the number of particles in each bunch given by N. We will then study the stability of infinitesimal deviations in particle distributions from a given equilibrium distribution. To do so, let the distribution of the m^{th} bunch be

$$\psi_{1,2}^{(m)} = \psi_0 + \Delta\psi_{1,2}^{(m)} \qquad , \qquad m = 1, 2, \cdots M \tag{33}$$

where the indices 1,2 refer to beam 1 and beam 2 respectively. Between collisions, the motion of individual bunches are decoupled,

$$\frac{\partial}{\partial s}\Delta\psi_{1,2}^{(m)} + \frac{1}{\beta}\,\frac{\partial}{\partial\phi}\Delta\psi_{1,2}^{(m)} = 0 \qquad , \qquad m = 1, 2, \cdots M \ . \tag{34}$$

To define the ordering of the collision sequence, we will make reference to the 1^{st} bunch of beam 1. When this bunch passes the collision point $s = 0$, the

$1, 2, .., M^{th}$ bunches in beam 1 collide respectively with the $1, 2, .., M^{th}$ bunches of beam 2. As the 1^{st} bunch of beam 1 proceeds to location $s = L$, the collisions occur between bunches $1, 2, .., M$ in beam 1 with bunches $M, 1, 2, ..., M-1$ in beam 2. When $s = ML$ (which is half the circumference of the storage ring), the whole cycle repeats and the collisions occur the same way as at $s = 0$.

The collision influence on bunch distributions can be described as follows. When the 1-st bunch of beam 1 is at the k-th collision point $s = kL$, we have

$$\Delta\psi_1^{(m)}|_{s=kL^+} - \Delta\psi_1^{(m)}|_{s=kL^-} = -A(J,\phi) \int_{-\infty}^{\infty} d\bar{y} H_1(y-\bar{y}) \int_{-\infty}^{\infty} d\bar{y}' \Delta\psi_2^{(n)}(\bar{y},\bar{y}') \quad (35)$$

together with another equation similar to (35) but with indices 1 and 2 exchanged and n and m exchanged. In Eq. (35) we have defined

$$A(J,\phi) = \frac{4\pi N r_e}{L_x \gamma} \sqrt{2J\beta} \ \sin\phi \ \psi_0'(J) \quad . \quad (36)$$

The indices n and m are related by the collision sequence; i.e. for $1 \leq k \leq M-1$, we have

$$n = \begin{cases} m + M - k & \text{if } 1 \leq m \leq k \\ m - k & \text{if } k+1 \leq m \leq M \quad . \end{cases} \quad (37)$$

The beam-beam collisions couple the distributions of all the bunches in both beams. It is possible to develop the transformation matrices describing the coupled system for half revolution around the storage ring. The stability of the system will then be given by the eigenvalues of this transformation. Instead of doing so, however, we will first make the change of variables

$$F_{1,2}^{(q)} \equiv \sum_{m=1}^{M} exp\left(i\frac{m}{M}2\pi q\right) \ \Delta\psi_{1,2}^{(m)} \quad , \quad q = 0, 1, \cdots, M-1 \quad . \quad (38)$$

Equation (38) relates the $2M$ quantities F's and the $2M$ quantities $\Delta\psi$'s. The problem then becomes the study of the stability of the F's.

The advantage of F's over $\Delta\psi$'s is that the F's are decoupled for different values of q's. Between collisions, we have

$$\frac{\partial}{\partial s} F_{1,2}^{(q)} + \frac{1}{\beta}\frac{\partial}{\partial \phi} F_{1,2}^{(q)} = 0 \quad . \tag{39}$$

For the k^{th} collision at $s = kL$, we have

$$\begin{aligned}
& F_1^{(q)} \mid_{s=kL+} - F_1^{(q)} \mid_{s=kL-} \\
& \qquad = -A(J,\phi)\ exp\left(i\frac{k}{M}2\pi q\right) \int d\bar{y}\ H_1(y-\bar{y}) \int d\bar{y}' F_2^{(q)} \\
& \bar{F}_2^{(q)} \mid_{s=kL+} - F_2^{(q)} \mid_{s=kL-} \\
& \qquad = -A(J,\phi)\ exp\left(-i\frac{k}{M}2\pi q\right) \int d\bar{y}\ H_1(y-\bar{y}) \int d\bar{y}'\ F_1^{(q)}
\end{aligned} \tag{40}$$

The index q is the coupled bunch mode number. For stability of the system, motions of all multi-bunch modes with different q's must be stable independently.

We now specify ψ_0 to be given by a water-bag model, Eq. (13), and Fourier decompose the F's according to

$$\begin{gathered}
F_j^{(q)}(J,\phi,s) = \delta\left(J - \frac{\epsilon}{2}\right) \sum_{\ell=-\infty}^{\infty} g_\ell^{(j,q)}(s)\ e^{i\ell\phi} \\
q = 0,1,2,\cdots M-1 \qquad , \qquad j = 1,2 \ .
\end{gathered} \tag{41}$$

The actions (39) and (40) can be described by matrix transformations on the g

coefficients. Defining the vector

$$G^{(q)} \equiv \begin{bmatrix} \vdots \\ g_1^{(1,q)} \\ g_0^{(1,q)} \\ g_{-1}^{(1,q)} \\ \vdots \\ g_1^{(2,q)} \\ g_0^{(2,q)} \\ g_{-1}^{(2,q)} \\ \vdots \end{bmatrix} \tag{42}$$

the transformation matrix between collision points is

$$\begin{bmatrix} R & 0 \\ 0 & R \end{bmatrix} \tag{43}$$

where R is the infinite dimensional matrix defined in Eq. (22) with μ the betatron phase advance between adjacent collision points. For the k^{th} collision, the matrix is

$$1 + \frac{2Nr_e}{\pi L_x \gamma}\sqrt{\frac{\beta^*}{\epsilon}}\ \exp\left(i\frac{k}{M}2\pi q\right)\ \begin{bmatrix} 0 & \mathcal{M} \\ \mathcal{M} & 0 \end{bmatrix} \tag{44}$$

where $\mathcal{M}$ is the matrix defined by Eq. (17). Multiplying matrices (43) and (44) over 1/2 ring circumference in proper sequence, the total transformation matrix can be obtained for each value of q. This is performed numerically for all multi-bunch modes. Stability is given by the condition that all eigenvalues of the matrices for each multi-bunch mode have an absolute value of 1.

The case in which there is only one bunch in each beam ($M = 1$) reproduces Figs. 1 to 3, as it should. Figure 4 gives the result when resonances up to order 2 (dipole and quadrupole instabilities) are included for cases $M = 1, 2, 3$ and 4. Figures 5 and 6 include resonances up to order 3 and 4, respectively. According to these results, the most stable choice of tune tends to be that slightly above an integer multiple of M.

6. Discussion

The beam-beam phenomenon is a difficult subject that probably involves more than one single effect. In this note we have analyzed it in terms of the coherent stability of the beams. Although, we do not pretend that this is the only important effect that occurs in the beam-beam phenomenon, we do suggest that coherent effects are indeed one of the most dominating beam-beam features.

In the analysis, we have assumed a water-bag model of the equilibrium beam distribution. This model is particularly simple to handle mathematically. As explained in Eq. (14), in doing so we have sacrificed a rigorous self-consistency. In addition, the system has a single frequency evaluated at the edge of the water-bag. This means that effects due to frequency spread are not included. All mode frequencies therefore are sharply defined lines. In particular, there is no Landau damping in this system.

The water-bag model has another disadvantage. It does not allow study of the radial modes in the bunch motions. As shown by Eqs. (15) and (41), the deviation in bunch distributions occur only at the edge of the water-bag, and therefore all radial modes degenerate into $\delta(J - \epsilon/2)$. Finally, we have considered only the vertical motion of the bunches. Horizontal motion and synchrotron motion would introduce many more resonances.

In spite of these limitations, the method used here to solve the Vlasov Equation takes full account of the discrete nature of the beam-beam kicks. This leads to a new method of calculating coherent beam-beam instabilities using a matrix mapping technique. It offers a simple description of the coherent beam-beam interaction and allows straightforward numerical calculations. In particular, all nonlinear resonances are treated simultaneously taking into account the coupling of the resonances.

One colliding beam phenomenon that has been observed experimentally is the beam size blow-up which occurs when intense beams are brought into collision.

In the present picture, this can perhaps be explained as follows. As beams collide, the equilibrium beam size does not change if the beam-beam motion is stable. As beam intensity increases so that an unstable region is entered, the beam size blows up but only by so much that the system becomes stabilized again. This means the value of ξ does not increase any more even if the beam intensity keeps on increasing. This behavior is similar to the bunch lengthening phenomenon observed in electron storage rings. From Eq. (32), it can be deduced that in the blown-up regime, the beam size scales approximately linearly with the beam intensity N. This agrees qualitatively with beam-beam experiments in electron storage rings.

Acknowledgement

We would like to thank A. Hofman, E. Keil and P. Morton for useful discussions, and Tor Raubenheimer for his help with numerical calculations and figures.

References

1. N. N. Chau and D. Potaux, Orsay Tech. Report 5-74 (1974) and 2-75 (1975), unpublished.
2. A. Piwinski, Proc. VIII Int. Conf. On High Energy Accel., CERN, 357 (1971).
3. A. Chao and E. Keil, CERN/ISR-TH/79-31 or PEP note 300 (1979), unpublished.
4. E. Keil, Proc. XI Int. Conf. On High Energy Accel., CERN, 759 (1980).
5. R. E. Mellen and R. H. Siemann, IEEE Trans. Nucl. Sci., NS-28, 2431 (1981).
6. Ya. S. Derbenev, Proc. III All Union Part. Accel. Conf., Moscow, 382(1973).
7. Ya. S. Derbenev, N. S. Dikansky, D. V. Pestrikov, Preprint 7-75, INPh, Siberian Division of USSR Academy of Science, 1972.
8. Y. Kamiya and A. W. Chao, SLAC / AP-8 (1983), unpublished.
9. R. Talman, Lecture at the High Energy Accelerator Summer School, Fermilab (1984).
10. The SPEAR Group, Proc. 9^{th} Int. Conf. on High Energy Accelerators, Stanford, 1974, p. 37.
11. A. Piwinski, AIP Proc. No. 57, Nonlinear Dynamics and the Beam-Beam Interaction, Brookhaven National Lab., 1979, Ed. M. Month and J. C. Herrera, p. 115.
12. J. Le Duff, et al., Proc. XI Int. Conf. on High Energy Accel., CERN, 707 (1980).
13. F. Sacherer, CERN/SI-BR/72-5 (1972), unpublished.
14. E. D. Courant and H. S. Snyder, Ann. Phys. 3, 1 (1958).

15. F. Amman and D. Ritson, International Conference on High Energy Accelerators, Brookhaven National Lab, 1961, p. 471.

Figure Captions

1. Stability diagrams in (ν_0, ξ_0) space, where ν_0 is the unperturbed tune for the storage ring and ξ_0 is the beam-beam strength parameter, for the cases with 1, 2, 3 and 4 bunches per beam. The beam bunches are regarded as rigid allowing only dipole coherent motions.

2. Stability diagrams for the case of one bunch per beam. In each of the four plots resonances up to order 2, 4, 6 and 8 are included, respectively.

3. (a) Stability diagrams for one bunch per beam including resonances through order 5. (b) Blow up of a portion of (a) showing some interference behavior between adjacent resonances.

4. Stability diagrams for the cases of 1, 2, 3 and 4 bunches per beam, taking into account dipole and quadrupole resonances.

5. Same as Fig. 4 but taking into account resonances up to order 3.

6. Same as Fig. 4 but taking into account resonances up to order 4.

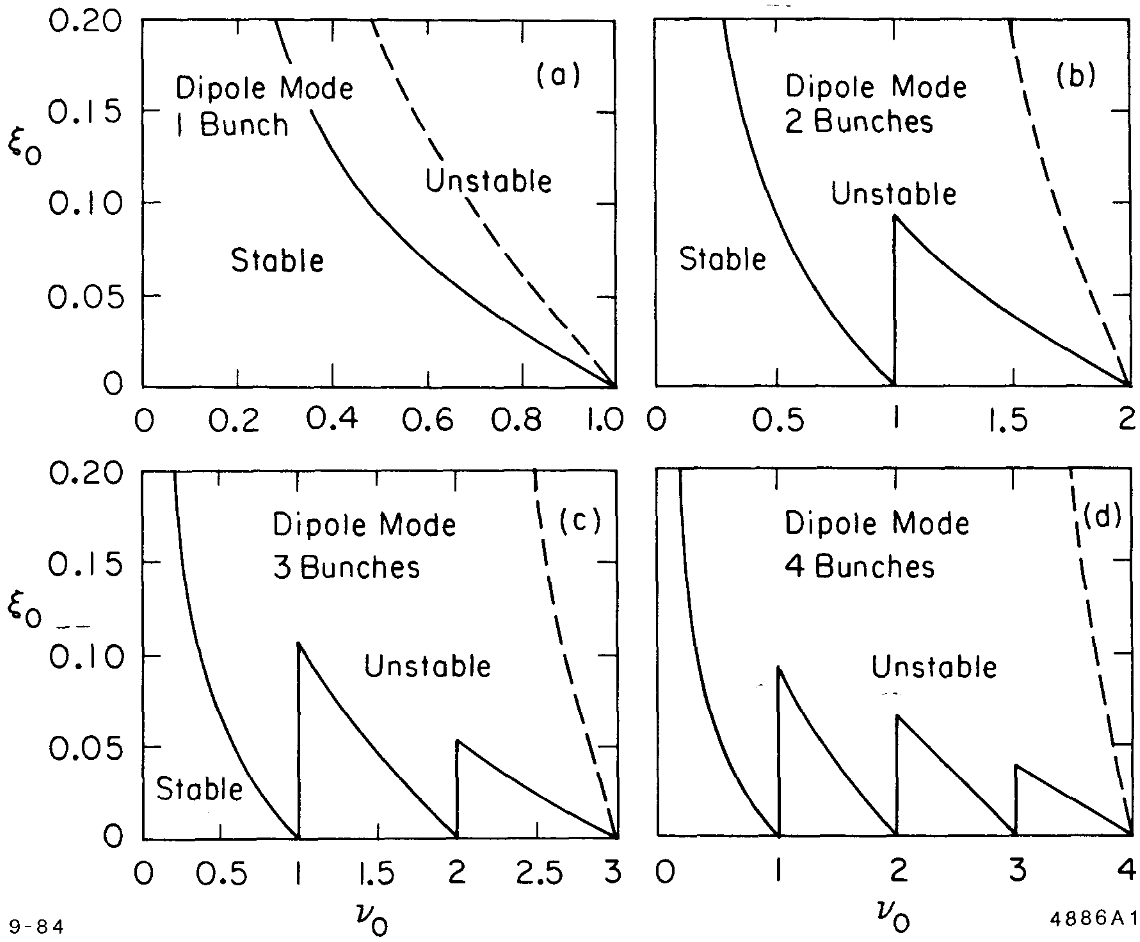
Dipole Mode
1 Bunch
(a)
Unstable
Stable
Dipole Mode
2 Bunches
(b)
Unstable
Stable
Dipole Mode
3 Bunches
(c)
Unstable
Stable
Dipole Mode
4 Bunches
(d)
Unstable
ξ_0
ν_0
9-84
4886A1

Fig. 1

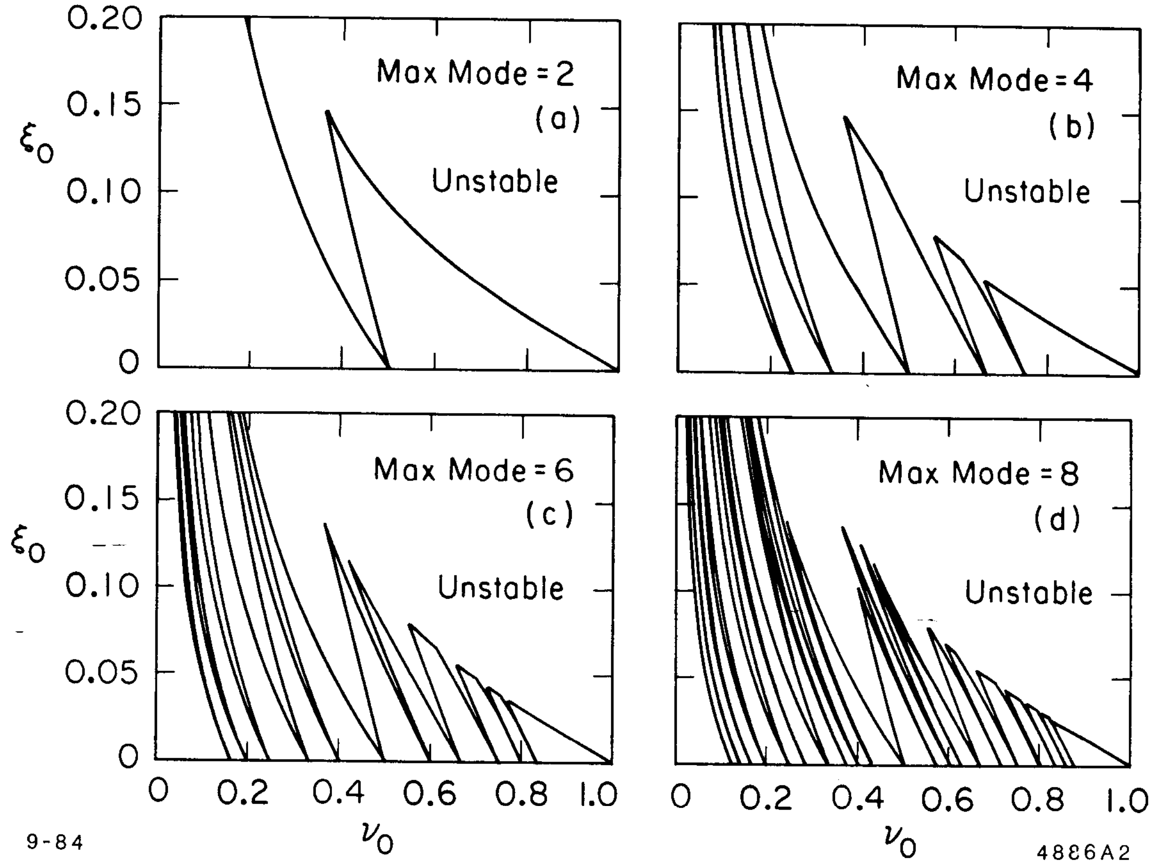

Max Mode = 2
(a)
Unstable
Max Mode = 4
(b)
Unstable
Max Mode = 6
(c)
Unstable
Max Mode = 8
(d)
Unstable
0.20
0.15
0.10
0.05
0
ξ_0
0
0.2
0.4
0.6
0.8
1.0
ν_0
9-84
4886A2

Fig. 2

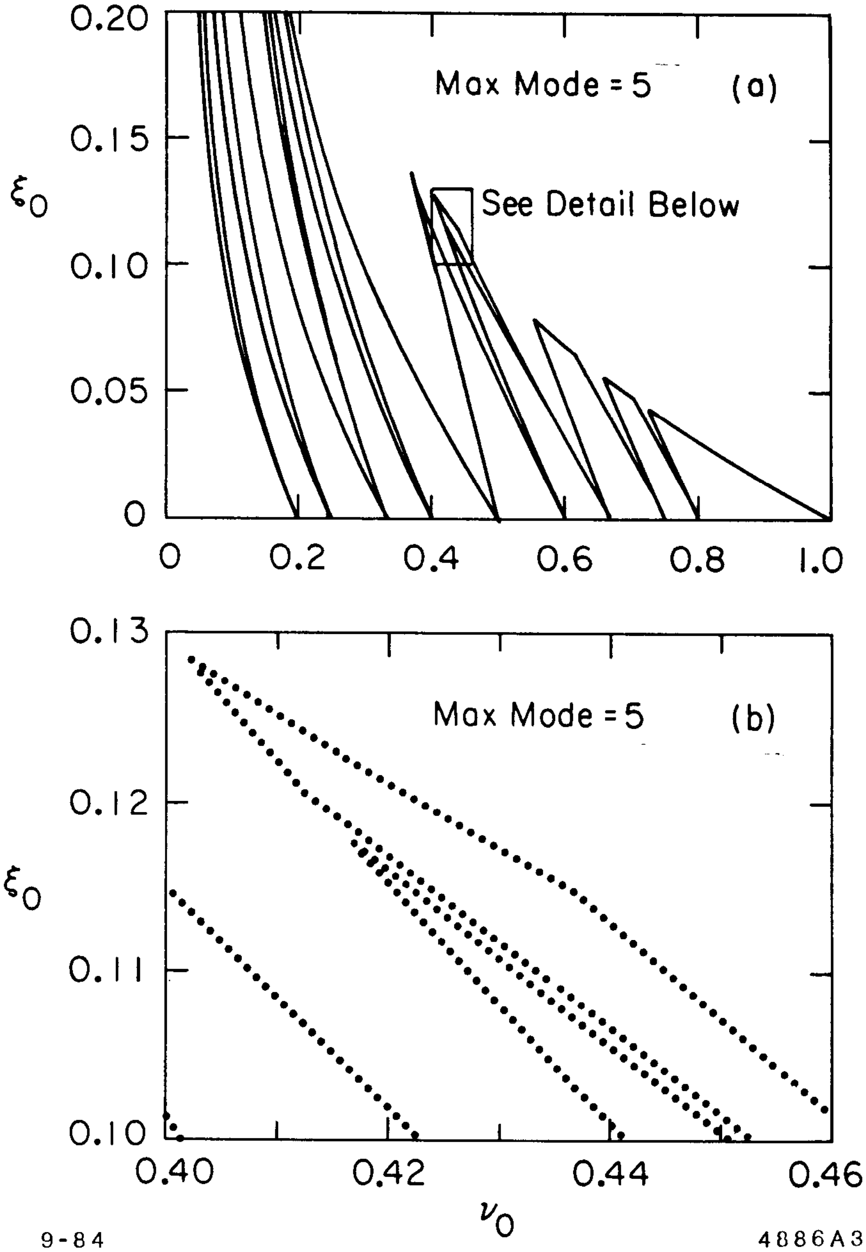

0.20
0.15
0.10
0.05
0
ξ_0
Max Mode = 5
(a)
See Detail Below
0
0.2
0.4
0.6
0.8
1.0
0.13
0.12
0.11
0.10
ξ_0
Max Mode = 5
(b)
0.40
0.42
0.44
0.46
ν_0
9-84
4886A3

Fig. 3

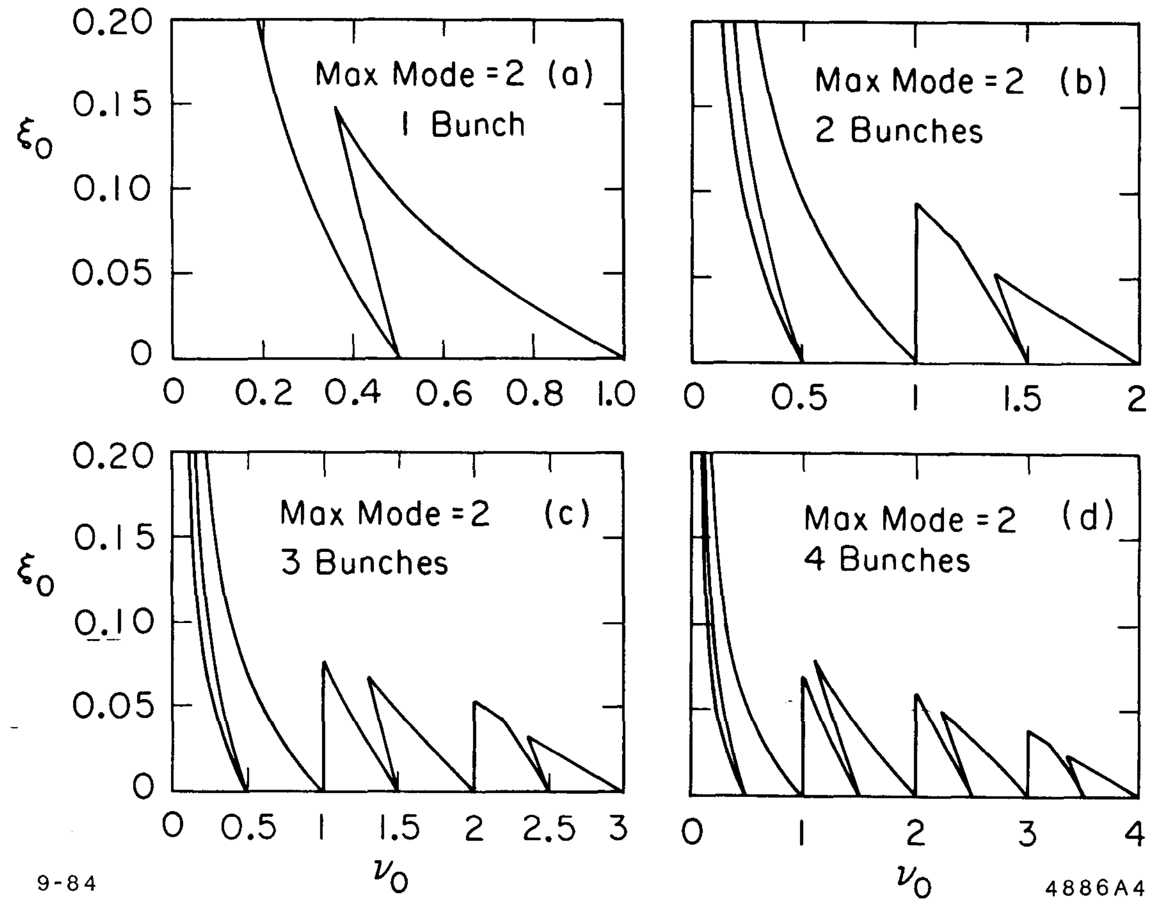

Max Mode = 2 (a)
1 Bunch
Max Mode = 2 (b)
2 Bunches
Max Mode = 2 (c)
3 Bunches
Max Mode = 2 (d)
4 Bunches
ξ_0
ν_0
0.20
0.15
0.10
0.05
0
0 0.2 0.4 0.6 0.8 1.0
0 0.5 1 1.5 2
0 0.5 1 1.5 2 2.5 3
0 1 2 3 4
9-84
4886A4

Fig. 4

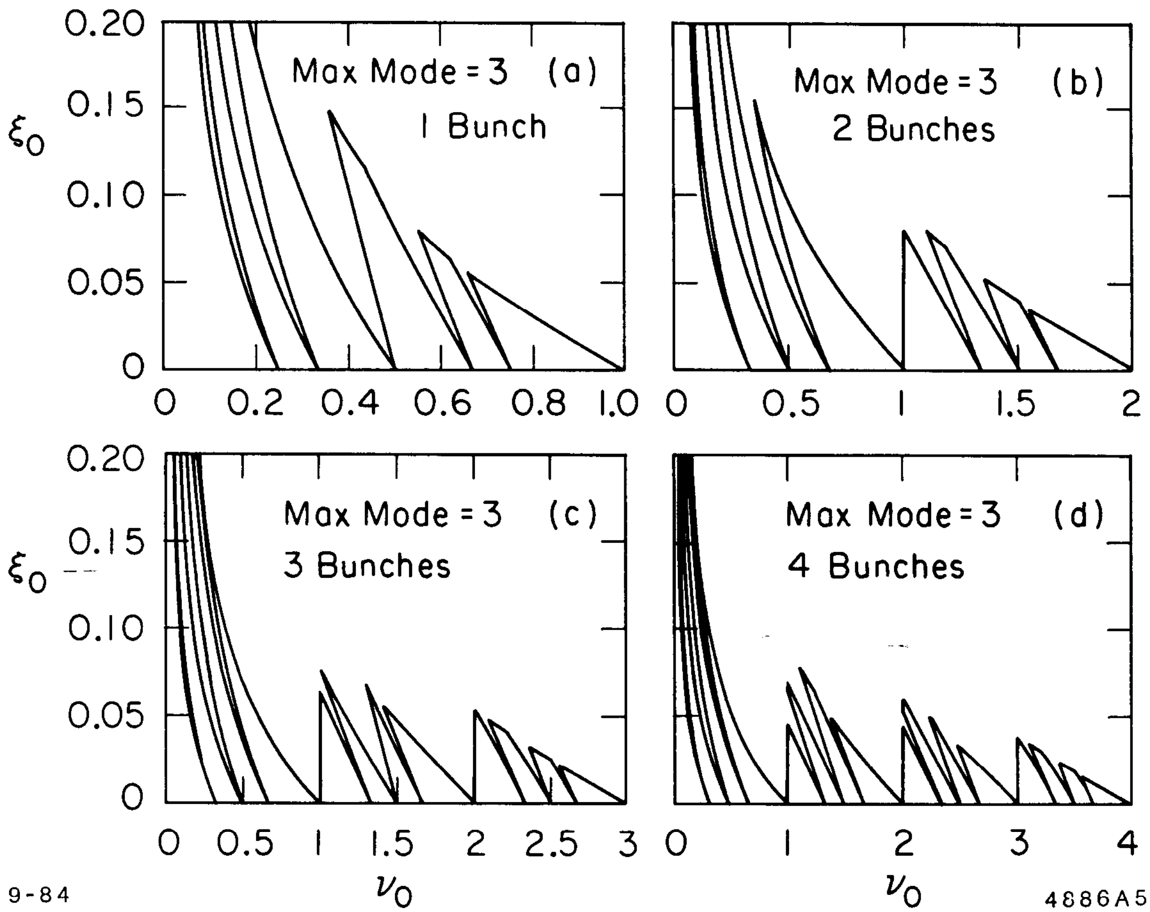
Max Mode = 3 (a)
1 Bunch
Max Mode = 3 (b)
2 Bunches
Max Mode = 3 (c)
3 Bunches
Max Mode = 3 (d)
4 Bunches
ξ_0
ν_0
0.20
0.15
0.10
0.05
0
0 0.2 0.4 0.6 0.8 1.0
0 0.5 1 1.5 2
0 0.5 1 1.5 2 2.5 3
0 1 2 3 4
9-84
4886A5

Fig. 5

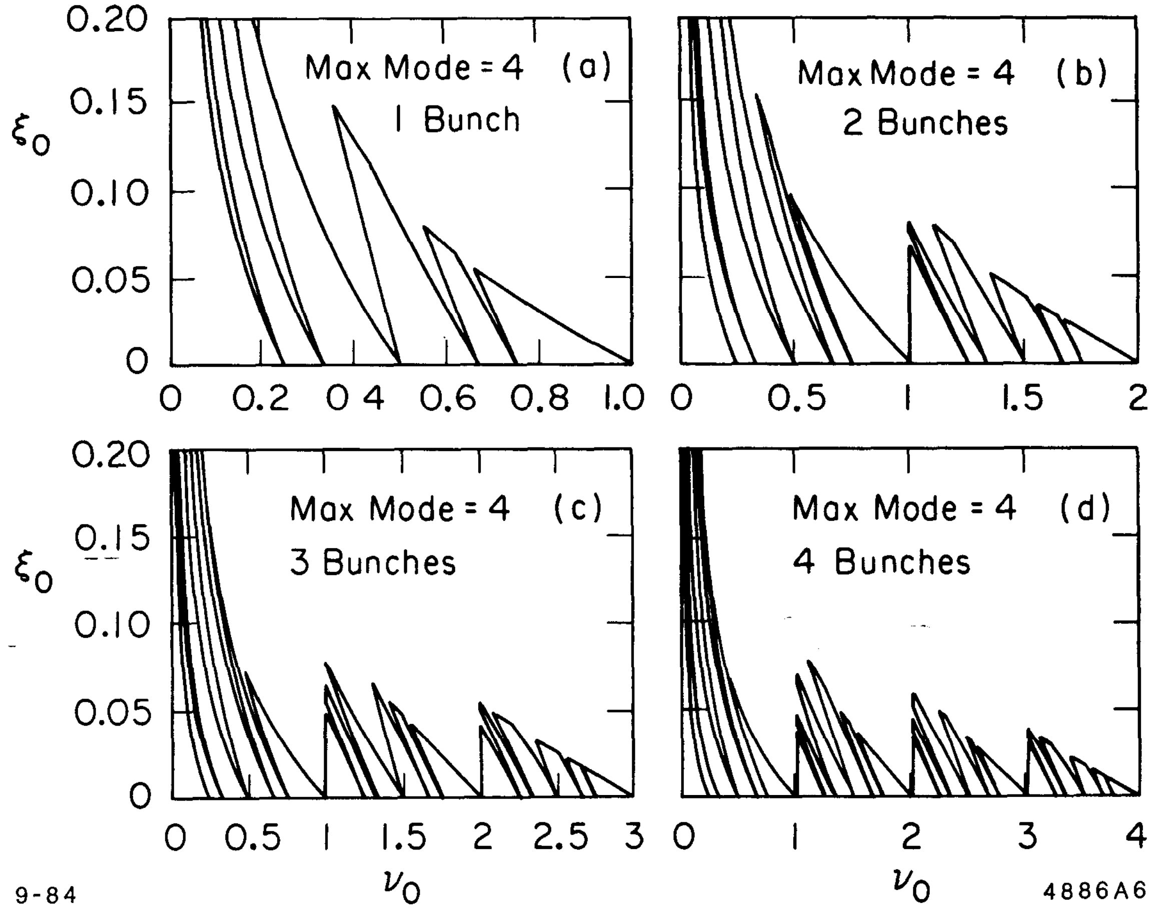
Max Mode = 4 (a)
1 Bunch
Max Mode = 4 (b)
2 Bunches
Max Mode = 4 (c)
3 Bunches
Max Mode = 4 (d)
4 Bunches
ξ_0
ν_0
0.20
0.15
0.10
0.05
0
0 0.2 0.4 0.6 0.8 1.0
0 0.5 1 1.5 2
0 0.5 1 1.5 2 2.5 3
0 1 2 3 4
9-84
4886A6

Fig. 6